Available online at www.sciencedirect.com
ScienceDirect
Chemical Physics Letters 430 (2006) 45–50
CHEMICAL PHYSICS LETTERS
www.elsevier.com/locate/cplett

Chirped modulation of molecular vibration in quinoidal thiophene after sub-5 fs excitation

Zhuan Wang [a], Tetsuo Otsubo [b], Takayoshi Kobayashi [a,c,d,e,*]

[a] Department of Physics, University of Tokyo, Hongo 7-3-1, Bunkyo, Tokyo 113-0033, Japan
[b] Department of Applied Chemistry, Hiroshima University, Higashi-Hiroshima 739-8527, Japan
[c] Department of Applied Physics and Chemistry, Institute of Laser Science, University of Electro-Communications, Chofugaoka 1-5-1, Chofu, Tokyo 182-8585, Japan
[d] Institute of Laser Engineering, Osaka University, Yamadakami 2-6, Suita 565-0871, Ibaraki 567-0047, Japan
[e] Department of Electrophysics, National Chiao Tung University, 1001 Ta Hsueh Road, Hsinchu 300, Taiwan

Received 1 June 2006; in final form 23 August 2006
Available online 30 August 2006

Abstract

Fourier transformation of the real-time trace of sub-5 fs pump-induced molecular vibration in quinoidal thiophene in solution revealed coupled modes to the electronic excitation at 206, 447, and 1466 cm^{-1}. Spectrogram analysis of 1466 cm^{-1} (C=C stretching) mode showed that the amplitude and frequency of the mode are modulated with another low-frequency mode at about 220 cm^{-1}, which is down chirped being induced by the coupling with modes of even lower frequency, resulting in the irreversible relaxation due to high mode density in the low-frequency range. This Letter thus reports on observation of the modulation of vibrational frequency with a chirped frequency.

1. Introduction

Thiophene-based oligomers can be readily synthesized [1–3] with different sizes and provide series of photophysical conjugated systems with different π-electron delocalization lengths. They have been extensively studied theoretically and experimentally for better understanding of the basic physical properties of polythiophene, which has been one of the best-known conjugated polymers since 1990s [4–14]. They have also been studied from the viewpoint of application as promising materials for devices [10,15–18] such as light-emitting diodes [19–21].

Vibrational spectroscopy of polythiophenes has shown [11] that they contain all-*s*-*trans* sequences of thiophene rings linked at α- and α′-positions with a distribution of conjugation lengths depending on both sequential length and torsion angles of thiophene rings. This is because the distribution of conjugation lengths has been ascribed to the existence of disordered structures in the polymer chain. Polythiophene has a nondegenerate ground state like *cis*-polyacetylene, which is different from *trans*-polyacetylene with a degenerate ground state. The optical properties of doped polythiophene have thus been discussed in terms of polarons and bipolarons [13–15], which are self-localized excitation in conjugated polymers. A study of the processes following the creation of electron and hole by photoexcitation is important to understand the mechanics of the generation of such nonlinear excitations.

In the present study, we have performed sub-5 fs spectroscopy of a derivative of quinoidal bithiophene [22] (Fig. 1) abbreviated as Bx-2, which is a good model molecule as a repeat unit of polythiophene with all-*s*-*trans*

* Corresponding author. Address: Department of Applied Physics and Chemistry and Institute of Laser Science, University of Electro-communications, Chofugaoka 1-5-1, Chofu, Tokyo 182-8585, Japan. Fax: +81 42 443 5825.
E-mail addresses: wang@ils.uec.ac.jp (Z. Wang), kobayashi@ils.uec.ac.jp (T. Kobayashi).

0009-2614/$ - see front matter © 2006 Elsevier B.V. All rights reserved.
doi:10.1016/j.cplett.2006.08.106

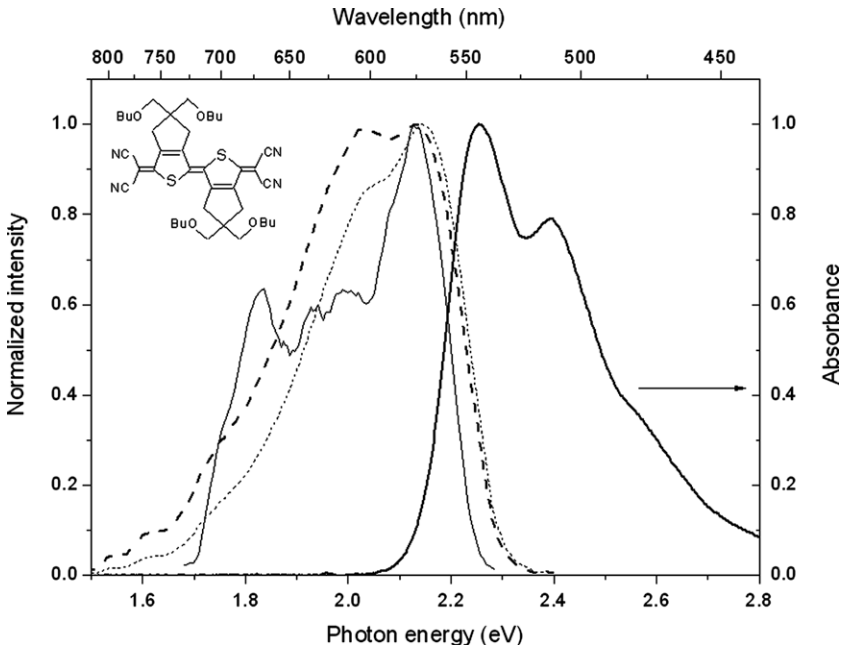

Fig. 1. Stationary absorption (thick solid), fluorescence (thick dashed), calculated stimulated emission (thin dotted), and laser (thin solid) spectra. The inset shows the quinoidal oligothiphene used in the present study.

conformation. We report here conformational changes of the molecular structure by torsion and a C=C stretching mode modulated by a down-chirped low-frequency mode after photoexcitation.

2. Experiment

As shown in Fig. 1, Bx-2 has dicyanomethylene groups at the terminal position and is a highly amphoteric redox molecule [22]. The stationary absorption and the fluorescence spectra were recorded with an absorption spectrometer (Shinmadzu, UV-3101PC) and a fluorophotometer (Hitachi, F-4500), respectively. The pump and probe pulses were both produced from a noncollinear optical parametric amplifier (NOPA) seeded by a white-light continuum [23–25]. The pulse of the NOPA output was compressed with a system composed of a pair of prisms and chirp mirrors [23–25]. The pump source of this NOPA system was a regenerative amplifier (Spectra Physics, Spitfire) with the following operating parameters: central wavelength: 790 nm, pulse duration: 50 fs, repetition rate: 5 kHz and average output power: 800 mW. A typical visible to near-infrared pulse was slightly shorter than 5 fs in duration and covered the spectral range of 520–750 nm, within which it carried a nearly constant spectral phase, indicating that the pulses were nearly Fourier-transform (FT) limited. The energy of the pump was ~30 nJ, which corresponds to the photon intensity of 1.2×10^{15} photons/cm^2. The probe pulse energy was ~6 nJ, five times weaker than the pump pulse. All the experiment was performed at room temperature (293 K). The quinoidal thiophene derivative was dissolved in tetrahydrofuran (THF), 0.02 wt%.

3. Results and discussion

3.1. Stationary spectra and real-time traces of absorbance change

The absorption and fluorescence spectra of the sample in THF solution and the laser spectra are shown in Fig. 1, together with the spectrum of stimulated emission, which is calculated from the spontaneous fluorescence spectrum by using the relationship between the Einstein A and B coefficients [26]. The absorption spectrum has two peaks, but the fluorescence gives a broad featureless spectrum. This may be explained in terms of geometrical relaxation just after photoexcitation. The molecule has a quinoidal structure in the S_0 ground state; it is more planar because of the C=C bond between the neighboring thiophene rings. In the S_1 state, the structure of the thiophene ring is expected to become aromatic and less planar. Then torsional motion is expected to take place in the structural relaxation process after photoexcitation.

Fig. 2a shows the probe delay time dependence of absorbance change (ΔA) induced by the sub-5 fs pump pulse at ten respective wavelengths. In the range shorter than 565 nm the absorbance change is mainly negative due to bleaching and/or stimulated emission. On the other hand, it is positive above 565 nm due to induced absorption. From the absorption spectrum and the stimulated emission spectrum calculated from the spontaneous fluorescence, the main contributions from the former and the latter are considered to be divided around 625 nm in case the transition dipole moments of absorption and stimulated processes are equal to each other.

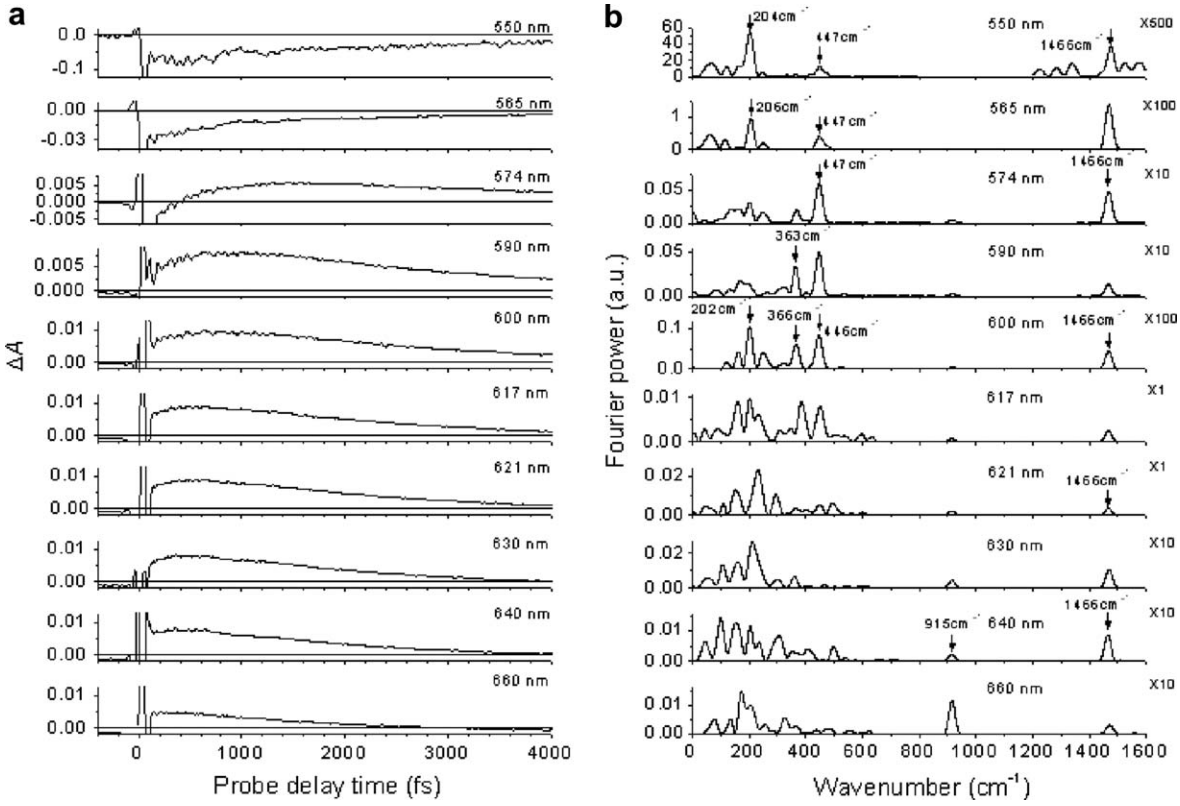

Fig. 2. Absorbance changes (a) as a function of the pump-probe delay time at ten wavelengths and FT power spectra (b) of oscillating components in the real-time trace. The FT power of each wavelength was amplified above 1200 cm^{-1} to observe the weak mode of 1466 cm^{-1}. The factors of multiplication are marked at the right margin.

Fig. 2b shows the Fourier transform of the corresponding real-time trace of the absorbance change probed at ten wavelengths in the range of pump–probe delay time from 150 to 2000 fs with respect to the cosine function. Two vibrational peaks are found in the FT power spectra around 915 and 1466 cm^{-1}. The former is assigned to the breathing mode from the solvent molecule of THF. The latter can be assigned to the C=C stretching mode of the solute molecule, which is also found in the Raman spectrum excited at 488 nm, as shown in Fig. 3, nearly resonant to the electronic transition of $S_1 \leftarrow S_0$. There are several other low-frequency modes around 206 and 447 cm^{-1} in the FT power spectra. They can be attributed to the torsional mode from the assignments of medium sized

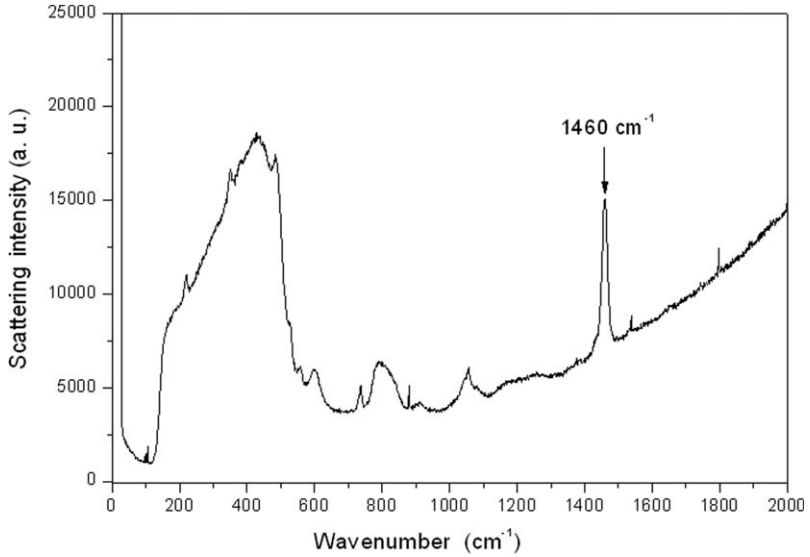

Fig. 3. Raman spectra of quinoidal oligothiophene under investigation, excited at 488 nm.

molecules similar to those of the present study. The characteristic feature of these vibrational modes is discussed later. Several low-frequency modes were also observed in the FT power spectra in the region of >617 nm, but clear assignment was impossible because poor reproducibility due to noise contamination.

3.2. Wave packet motions of vibrational modes on the ground state potential surface

The FT amplitudes of the torsional modes at 206 and 447 cm^{-1} were compared with the transient ΔA spectrum in the shorter wavelength range, as shown in Fig. 4. The ΔA spectrum was averaged over the pump-probe delay time ranging from 150 to 2000 fs, which is equal to that in the FT analysis. These two FT amplitudes fit the bleaching signal of the ΔA spectrum very well below 570 nm. However, it shows a poor fit in the range above 570 nm. This is because the FT amplitudes at 206 and 447 cm^{-1} were nearly zero and the ΔA signals were positive, due to induced absorption. It indicates that the two modes are mainly coupled with the wave packet on the electronic ground state. At the same time, the FT amplitude at the 206 cm^{-1} mode is larger than that at 446 cm^{-1}, and the former fits the bleaching signal of ΔA better, which shows that the former vibrational mode is more strongly coupled with the ground state than the latter mode.

3.3. Spectrogram analysis of the C=C stretching mode

The time-frequency analysis was performed using spectrograms to study the dynamic behavior of the C=C stretching mode. The window function used for the calculation of the spectrogram was a Blackman type with full width at half maximum (FWHM) of 300 fs and the corresponding integration FWHM bandwidth is 111 cm^{-1} in frequency domain. The spectrograms were calculated at several wavelengths and an example of 617 nm is shown in Fig. 5. This clearly exhibits characteristic features of frequency and amplitude modulations. Furthermore, the periods of the frequency and the amplitude modulations both changed with time; namely, the modulation frequency decreased with time. We call this slow-down process 'negative chirp', taken from the definition of this term.

Chirp modulation is studied by the following response functions of delay time against instantaneous frequency [27].

$$M_a(t) = e^{-t/T_r}(1 - e^{-t/T_g})\left[a + b\cos\left(\frac{2\pi}{T_0 + kt} + \varphi_0\right)\right] \quad (1)$$

$$M_f(t) = wn_0 + (1 - e^{-t/T_g})\left[a + b\cos\left(\frac{2\pi}{T_0 + kt} + \varphi_0\right)\right] \quad (2)$$

The chirped modulation functions were convoluted with the laser response function to fit the results to simulation. Here, T_r is the relaxation time, T_g is a phenomenological time constant to take care of artifact induced by the lack of signal at the negative delay times due to the finite gate width of the spectrogram near zero delay, wn_0 is a constant to get the average frequency of the C=C stretching mode, T_0 is the initial period, k is the chirp rate of the molecular vibration frequency, φ_0 is the initial phase of the modulation frequency and a and b are fitting constants. Subscripts a and f indicate amplitude and frequency modulations, respectively. We only made a fitting to the experimental results in the range of 140–1100 fs because a weak oscillation with a smaller signal-to-noise ratio was observed after 1100 fs. The best parameters of the results of fitting, shown in Fig. 5, are listed in Table 1. The initial period and the chirp rate show the essential information on the modulations. The initial periods of 160 and 140 fs correspond to the modulation frequencies of 208 and 238 cm^{-1}, which are damped to 115 and 108 cm^{-1} after 1 ps with the chirp

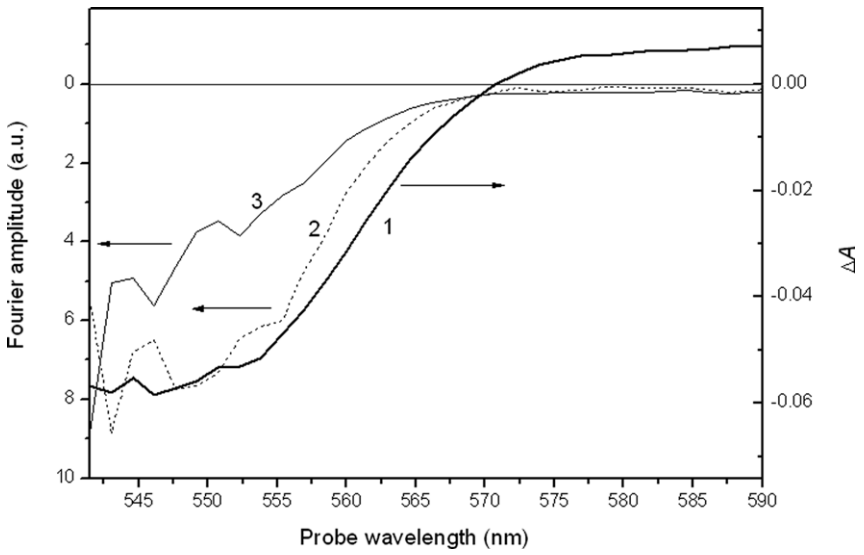

Fig. 4. (1) Absorbance change spectrum and FT amplitude spectra at (2) 206 and (3) 446 cm^{-1}.

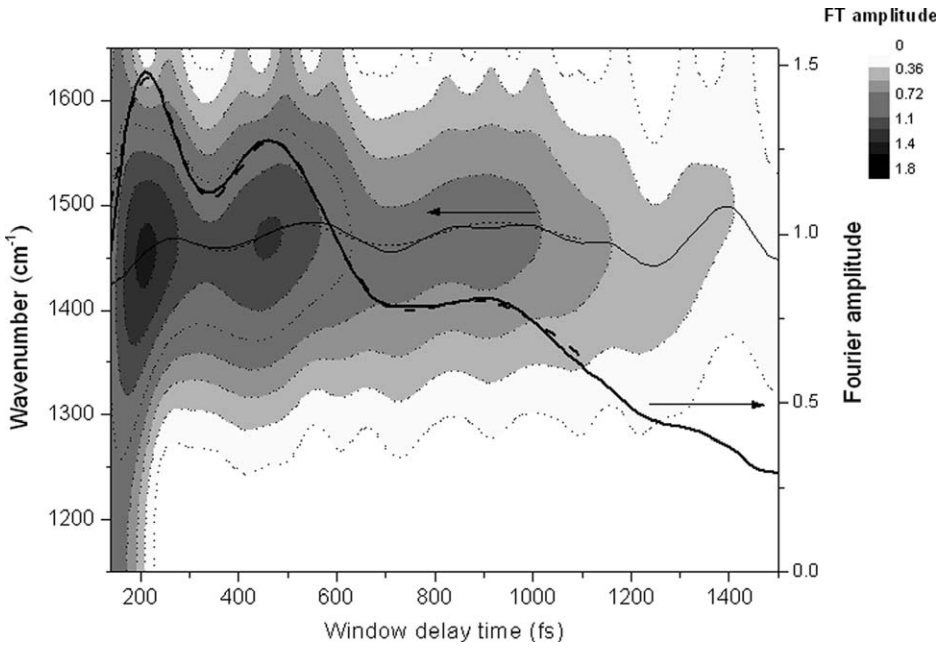

Fig. 5. Contour map of the spectrogram for the real-time data calculated at 617 nm. Frequency peaks around 1466 cm^{-1} (C=C stretching) mode (thin solid), FT amplitude of these frequency peaks (thick solid), and the results of fitting to these two (thin and thick dashed, respectively).

Table 1
Fitting parameters to $M_a(t)$ and $M_f(t)$ describing the damped modulations to the frequency and intensity[a]

Modulations	T_g (fs)	T_r (fs)	wn_0 (cm^{-1})	a/b	T_0 (fs)	$1/(cT_0)$ (cm^{-1})[b]	k (fs^{-1})	φ_0 (π)
Frequency	120		1356	11.545	160	208	0.13	−0.6
Amplitude	110	950		7.917	140	238	0.17	−0.4

[a] See text for the meaning of parameters.
[b] c is the light velocity in vacuum.

rates of 0.13 and 0.17 fs^{-1}, respectively. The parameters of the frequency and amplitude modulations are close to each other; this indicates that the modulations originate most probably from the same mode of ~220 cm^{-1}. The chirping of the frequency and amplitude modulations of 1466 cm^{-1} (C=C stretching) mode is probably caused by vibrational energy relaxation to modes of lower frequencies, to be explained as follows.

The chirped modulation modes are coupled to those of even lower frequency and no retrieval takes place due to a high mode density in the system and/or relaxation to vibrational modes of lower frequencies and translational motions of solvent molecules. Thus the chirped vibration is considered to be composed of many modes with distributed frequencies. This is the reason why 220 cm^{-1} does not appear in the Fourier power spectra in Fig. 2b unlike other low-frequency modes of 206 and 447 cm^{-1}.

The phase of the 1466 cm^{-1} mode at this wavelength was clearly determined to be 0.06π by the FT analysis of the real-time trace, which indicates that the C=C stretching is dominantly from the excited state [30]. On the other hand, it is difficult to determine the phase of the chirped modulations precisely, because of the arithmetic of the spectrogram itself. It is necessary to calculate the spectrogram from zero delay to determine the phase of the vibration precisely. However, the amplitude and instantaneous frequency of the C=C stretching mode near zero delay are deformed because there is no signal in the negative delay region. Hence, it is difficult to determine the phase of molecular vibration and the chirping frequency. Possible deviation from the linear chirp assumption also impairs definite determination of the phase. It is also likely that the low-frequency mode around 220 cm^{-1} is not totally symmetric; nor is it Raman active, resulting in the absence of the real-time trace, while it can modulate the frequency and amplitude of the Raman-active C=C stretching mode at 1466 cm^{-1}.

The bithiophene derivative studied in the present paper has only five C=C bonds in the system, and there might be raised such an argument that it is not a polynene but is just a molecule. However, we have studied three polyacetylene derivatives and found that the soliton size in the poly-[[*o*-(trimethyl-silyl)phenyl]acetylene] is $(4.5 \pm 0.5)a$, where a is the length of the repeat unit [28,29]. It is well characterized for three different polyacetylene derivatives and well discussed in terms of confined solitons. Polarons are even smaller than solitons because of their intrinsic properties of such nonlinear excitation. The size is therefore

considered to be even shorter than the 5 repeat units in Bx-2 studied in the present paper.

3.4. Conclusion

Molecular chain torsion was observed after the quinoidal thiophene derivative was excited. This indicates that a thiophene derivative changes structure from quinoidal to aromatic after excitation. Both frequency and amplitude of the excited state wave packet of the C=C stretching mode are found to be modulated by a low and chirped frequency mode. This also identifies the geometrical relaxation relevant to polaron and/or bipolaron formation in this quinoidal thiophene derivate.

Acknowledgements

The authors are grateful to Mr. Akira Ozawa for his help in the pump-probe experiment. This research is partly supported by a Grant-in-Aid for Specially Promoted Research (#14002003), the program for the Promotion of Leading Researches in Special Coordination Funds for Promoting Science and Technology from the Ministry of Education, Culture, Sports, Science and Technology. This work is also supported partly by the ICORP program of Japan Science and Technology Agency (JST) and the grant MOE ATU Program in NCTU.

References

[1] T. Izumi, S. Kobashi, K. Takimiya, Y. Aso, T. Otsubo, J. Am. Chem. Soc. 125 (2003) 5286.
[2] T.M. Pappenfus, R.J. Chesterfield, C.D. Frisbie, K.R. Mann, J. Casado, J.D. Raff, L.L. Miller, J. Am. Chem. Soc. 124 (2002) 4184.
[3] H. Higuchi, T. Nakayama, H. Koyama, J. Ojima, T. Wada, H. Sasabe, Bull. Chem. Soc. Jpn. 68 (1995) 2363.
[4] T. Kobayashi, M. Yoshizawa, U. Stamm, M. Taiji, M. Hasegawa, J. Opt. Soc. Am. B 7 (1990) 1558.
[5] U. Stamm, M. Taiji, M. Yoshizawa, K. Yoshino, T. Kobayashi, Mol. Cryst. Liq. Cryst. A 182 (1990) 147.
[6] R.N. Marks et al., Chem. Phys. 227 (1998) 49.
[7] M. Muccini, E. Lunedei, A. Bree, G. Horowitz, F. Garnier, C. Taliani, J. Chem. Phys. 108 (1998) 7327.
[8] F. Garnier, R. Hajlaoui, A. Yassar, P. Srivastava, Science 265 (1994) 1684.
[9] L.L. Miller, Y. Yu, E. Gunic, R. Duan, Adv. Mater. 7 (1995) 547.
[10] D. Fichou, J.-M. Nunzi, F. Charra, N. Pfeffer, Adv. Mater. 6 (1994) 64.
[11] Y. Furukawa, M. Akimoto, I. Harada, Synth. Met. 18 (1988) 151.
[12] A. Yang, S. Hughes, M. Kuroda, Y. Shiraishi, T. Kobayashi, Chem. Phys. Lett. 280 (1997) 475.
[13] A.J. Heeger, S. Kivelson, J.R. Schrieffer, W.-P. Su, Rev. Mod. Phys. 60 (1988) 781.
[14] H. Kiess (Ed.), Conjugated Conducting Polymers, Springer-Verlag, Berlin, 1992.
[15] G. Horowitz, D. Fichou, X.Z. Peng, Z.G. Xu, F. Garnier, Solid State Commun. 72 (1997) 381.
[16] A. Dodabalapur, L. Torsi, H.E. Katz, Science 268 (1995) 270.
[17] N. Noma, T. Tsuzuki, Y. Shirota, Adv. Mater. 7 (1995) 647.
[18] R. Hajlaoui, G. Horowitz, F. Garnier, Adv. Mater. 9 (1997) 389.
[19] F. Geiger, M. Stoldt, H. Schweizer, P. Bauerle, E. Umbach, Adv. Mater. 5 (1993) 922.
[20] T. Noda, H. Ogawa, N. Noma, Y. Shirota, Adv. Mater. 9 (1997) 720.
[21] K. Uchiyama, K. Akimichi, S. Hotta, H. Noge, H. Sakaki, Synth. Met. 63 (1994) 57.
[22] T. Takahashi, K. Matsuoka, K. Takimiya, T. Otsubo, Y. Aso, J. Am. Chem. Soc. 127 (2005) 8928.
[23] A. Shirakawa, I. Sakane, T. Kobayashi, Opt. Lett. 23 (1998) 1292.
[24] A. Shirakawa, I. Sakane, M. Takasaka, T. Kobayashi, Appl. Phys. Lett. 74 (1999) 2268.
[25] A. Baltuska, T. Kobayashi, Appl. Phys. B: Lasers Opt. 75 (2002) 427.
[26] R. Loudon, The Quantum Theory of Light, Clarendon Press, Oxford, 1973, p. 39.
[27] S. Pedersen, L. Banares, A.H. Zewail, J. Chem. Phys. 97 (1992) 8801.
[28] S. Takeuchi, M. Yoshizawa, T. Masuda, T. Higashimura, T. Kobayashi, IEEE J. Quant. Elect. 28 (1992) 2508.
[29] S. Takeuchi, T. Masuda, T. Kobayashi, Phys. Rev. B 52 (1995) 7166.
[30] H. Kano, T. Saito, T. Kobayashi, J. Phys. Chem. A 106 (2002) 3445.